Transport in Porous Media (2022) 144:641–667
https://doi.org/10.1007/s11242-022-01828-x

Analytical Solutions to Three-Dimensional Reactive Contaminant Transport Problems Involving Point, Line, and Area Sources

Jhansi Sangani[1] · Antriksh Srivastava[1] · Venkatraman Srinivasan[1]

Received: 7 January 2022 / Accepted: 7 July 2022 / Published online: 3 August 2022

Abstract
Screening tools such as BioScreen, BioChlor, ATRANS, AT123D-AT, ArcNLET, and Hydroscape are routinely employed to simulate the three-dimensional transport of reactive contaminants in groundwater. These tools estimate contaminant plume concentrations either using exact semi-analytical solutions or the approximate closed-form Domenico analytical solution. Semi-analytical solutions involve numerical integration procedures that can be mathematically challenging and computationally demanding. To overcome this, screening tools often use the approximate closed-form Domenico solution. However, the approximate Domenico solution introduces significant errors under realistic values of longitudinal dispersion, especially at plume locations beyond the advective front. Recently, an improved closed-form approximation to the three-dimensional reactive transport problem was developed using the concept of characteristic residence time. However, this solution was only applicable for a rectangular area source subject to a Dirichlet boundary condition. This severely restricts the use and applicability of the closed-form approximate solution to solve practically relevant simplified groundwater contaminant transport problems. Here, we present a library of six exact semi-analytical solutions for point, line, and area sources (three source geometries) under Dirichlet and Cauchy boundary conditions (two boundary conditions). Additionally, we develop approximate closed-form analytical solutions for all six solutions using the characteristic residence time concept. Our approximate solutions match well with the exact solutions under a wide range of parameter and domain conditions. We extend our analytical solutions to include the effects of linear equilibrium sorption, source decay, and pulse source input. Our analytical solution library facilitates the application of screening tools for a wide range of practically relevant simplified groundwater reactive contaminant transport problems.

Keywords Analytical solution · Approximate solution · Groundwater · Contaminant transport · Screening tool

✉ Venkatraman Srinivasan
venkatraman@iitm.ac.in

[1] Department of Civil Engineering, Indian Institute of Technology Madras, Chennai, India

1 Introduction

Analytical and semi-analytical solutions are often employed in screening tools for groundwater contamination studies (Newell et al. 1996; Aziz et al. 2000; Neville 2005; Burnell et al. 2012; Rios et al. 2013; Funk et al. 2017). Transport problems solved by analytical and semi-analytical solutions typically assume homogeneous porous media aquifer characteristics, steady and uniform flow conditions, simplified first-order decay reaction kinetics, and linear equilibrium adsorption (Wexler 1992; Srinivasan et al. 2007; Wang and Wu 2009).

While closed-form analytical solutions enable direct computation of plume solute concentrations, semi-analytical solutions require numerical integration procedures to compute final plume concentrations (Sangani and Srinivasan 2021). Numerical integration introduces numerical errors and increases computational times, making them cumbersome to use in screening tools (Srinivasan et al. 2007; Sangani and Srinivasan 2021). Additionally, integral evaluations involved in semi-analytical solutions require special techniques to obtain desired accuracy (Karanovic et al. 2007; Wang et al. 2011; Burnell et al. 2012).

The closed-form analytical solution for the one-dimensional contaminant transport problem with advection and dispersion in a semi-infinite domain was first presented by Ogata and Banks (1961). The solution of Ogata and Banks (1961) was applicable for a conservative tracer subject to a Dirichlet boundary condition. Bear (1972) extended the Ogata and Banks (1961) solution to include the effect of first-order decay. Later, Cleary and Ungs (1978) added linear equilibrium sorption to the Bear (1972) solution. van Genuchten (1981) presented the analytical solution for the transport problem solved by Cleary and Ungs (1978) under the Cauchy boundary condition. Additionally, van Genuchten (1981) presented solutions for one-dimensional transport problems involving nonzero initial conditions, exponential source decay, and zero-order production.

Using Laplace transforms, Wilson and Miller (1978) presented a semi-analytical solution for the two-dimensional transport of a non-conservative contaminant subject to a point source Dirichlet boundary condition. Later, (Sagar 1982) derived a semi-analytical solution to the three-dimensional transport problem subject to an area source with Dirichlet boundary condition. However, the solution presented by (Sagar 1982) was for a conservative contaminant. Using a similar approach, Batu and van Genuchten (1990) developed solutions for the transport problem considered by Wilson and Miller (1978) with Cauchy boundary conditions. Leij et al. (1991) extended the Sagar (1982) solution to include semi-analytical solutions for a non-conservative decaying source under Dirichlet and Cauchy boundary conditions. The Leij et al. (1991) solutions also included a zero-order production term.

Wexler (1992) derived semi-analytical solutions to three-dimensional contaminant transport problems for point, line, and area sources subject to Dirichlet boundary conditions. Solutions presented by Wexler (1992) included the effects of the plume and source decay. Chrysikopoulos (1995); Sim and Chrysikopoulos (1999) presented semi-analytical solutions for the three-dimensional contaminant transport of a rectangular area source where the flow is parallel to the source plane.

Wang and Wu (2009) compiled a library of solutions for the three-dimensional transport of contaminants subject to Dirichlet boundary conditions for point, line, and area sources. Wang and Wu (2009) also included solutions where the orientation of the patch source was parallel to the flow direction, and the shape of the source was a parallelepiped instead of a rectangle. The semi-analytical solutions library compiled by Wang and Wu (2009) can be numerically integrated using standard Gauss–Legendre quadrature techniques to obtain accurate estimates of plume concentrations (Karanovic et al. 2007).

Using Green's function method, Yeh (1981) presented a set of solutions for the fate and transport of groundwater contaminants for point, line, and area (rectangle) sources under Dirichlet boundary conditions. Yeh (1981) considered contaminants undergoing first-order decay and linear equilibrium sorption with the aquifer media. The two- and three-dimensional solutions presented by Yeh (1981) were computationally demanding and prone to errors (Burnell et al. 2012).

Ellsworth and Butters (1993) derived solutions for the three-dimensional transport of contaminants where the flow direction was not necessarily aligned with the Cartesian coordinate system. Using Bessel and modified Bessel functions, Leij et al. (1993) presented semi-analytical solutions for the three-dimensional transport of reactive contaminants subject to non-equilibrium adsorption kinetics. Using Green's function method, Leij et al. (2000) extended the area (rectangular) source transport problem of Yeh (1981) to include source characterizations where the rectangular source was parallel to the advective flow direction. Additionally, Leij et al. (2000) also included zero-order production terms in the transport problem. These additions help in modeling the leaching of non-aqueous phase solutes in groundwater.

Integrating semi-analytical solutions such as those derived from Green's function method can result in errors due to slow convergence and the presence of oscillatory terms (Burnell et al. 2012). To overcome this, Karanovic et al. (2007); Wang et al. (2011) employed the Gauss–Legendre quadrature integration technique. Burnell et al. (2012) applied the Romberg integration technique coupled with variable time stepping and an integral partitioning approach to minimize the errors of the semi-analytical solutions. However, these semi-analytical solutions are computationally demanding compared to closed-form analytical solutions.

Domenico and Robbins (1985) presented a closed-form approximate analytical solution (Domenico solution) for the three-dimensional contaminant transport problem considered by Sagar (1982). This was accomplished by artificially removing the transverse dispersion terms from the integration and independently integrating the remaining longitudinal advection–dispersion term (Srinivasan et al. 2007). Later, Domenico (1987) extended this approach and developed a closed-form approximate solution for a decaying contaminant. Martin-Hayden and Robbins (1997) improved the accuracy of the Domenico (1987) approximation near the source by including the expanded form of longitudinal dispersion term as given in Ogata and Banks (1961).

Several studies investigated the errors associated with the Domenico approximation. While West and Kueper (2004) showed that the errors in the Domenico solution could be up to 50% along the plume centerline, Guyonnet and Neville (2004) suggested that the errors will be higher away from the plume centerline. Srinivasan et al. (2007) presented a mathematical analysis of the errors associated with the Domenico solution. Using model sensitivity simulations, Srinivasan et al. (2007) showed that the errors are higher under i) large values of longitudinal dispersivity and ii) at plume locations beyond the advective front. Similar conclusions were also obtained by West et al. (2007). Additionally, Srinivasan et al. (2007) mathematically demonstrated that the Domenico solution transforms into an exact closed-form analytical solution under zero longitudinal dispersivity.

Sangani and Srinivasan (2021) developed an improved analytical approximation (S &S solution) to the Domenico solution by introducing the concept of characteristic residence time. They showed that the Domenico approximation fails to include the effect of transport due to longitudinal dispersion, and by explicitly accounting for longitudinal dispersive transport in the characteristic residence time representation, the errors in S &S approximation are significantly reduced, especially at plume locations beyond the advective front.

However, the approximate Domenico and S &S solutions are only valid for transport problems involving a rectangular area source subject to the Dirichlet source boundary condition. This severely restricts the use and applicability of the closed-form approximate solutions to solve practically relevant simplified groundwater contaminant transport problems.

Exact semi-analytical solutions exist for area source geometry under Dirichlet and Cauchy boundary conditions (Table 1). However, solutions with point and line source geometries are only available under Dirichlet boundary conditions. Presently, there are no exact semi-analytical solutions for point and line sources subject to a Cauchy source boundary condition. Closed-form approximate analytical solutions are only available for the area source geometry under Dirichlet boundary conditions. The available set of exact semi-analytical solutions and approximate closed-form analytical solutions are not complete to model point, line, and area source geometries under both Dirichlet and Cauchy boundary conditions.

The objectives of this paper are:

1 Derive exact semi-analytical solutions for two-dimensional and three-dimensional transport problems with point and line source geometries under the Cauchy boundary condition.
2 Develop closed-form approximate analytical solutions for two-dimensional and three-dimensional transport problems with point and line source geometries under Dirichlet and Cauchy boundary conditions and area source geometry under the Cauchy boundary condition.
3 Extend solutions for exact and approximate solutions that include the effects of linear equilibrium sorption and pulse source boundary conditions.

2 Analytical Solutions for Point, Line, and Area Sources

The governing equation describing the fate and transport of a groundwater solute undergoing one-dimensional advection, three-dimensional dispersion, linear equilibrium sorption, and first-order decay is given as:

$$\frac{\partial C}{\partial t} = -v_x \frac{\partial C}{\partial x} + D_x \frac{\partial^2 C}{\partial x^2} + D_y \frac{\partial^2 C}{\partial y^2} + D_z \frac{\partial^2 C}{\partial z^2} - kC \tag{1}$$

where C is the solute concentration [mg L^{-1}], v_x is the advection velocity in the x direction [m day^{-1}], $D_x = D^* + v_x\alpha_x$, $D_y = D^* + v_y\alpha_y$, and $D_z = D^* + v_z\alpha_z$ are the dispersion coefficients [m^2 day^{-1}] in x, y, and z directions, respectively, D^* is the molecular diffusion coefficient [m^2 day^{-1}], α_x, α_y, and α_z are the dispersivities [m] (caused by mechanical dispersion) in x, y, and z directions, respectively, and k is the first-order decay coefficient [day^{-1}].

Typically, $D^* \ll D_x$, D_y, and D_z and is usually neglected. This simplifies the governing Eq. 1 to:

$$\frac{\partial C}{\partial t} = -v_x \frac{\partial C}{\partial x} + v_x\alpha_x \frac{\partial^2 C}{\partial x^2} + v_x\alpha_y \frac{\partial^2 C}{\partial y^2} + v_x\alpha_z \frac{\partial^2 C}{\partial z^2} - kC \tag{2}$$

The initial condition for a solute-free groundwater aquifer is given as:

Table 1 Summary of exact and approximate analytical solutions for one-, two-, and three-dimensional solute transport in groundwater. Bold text indicates the solutions developed in this paper

Source	Point	Point	Line	Point	Line	Area
Exact						
Dirichlet	Closed-form[a]	Single-integral[b]	Single-integral[b]	Single-integral[c]	Single-integral[c]	Single-integral[c]
Cauchy	Closed-form[a]	Single-integral[g]	Single-integral[g]	Single-integral[g]	Single-integral[g]	Single-integral[e]
Approximate						
Dirichlet	Closed-form[a]	Closed-form[g]	Closed-form[g]	Closed-form[g]	Closed-form[g]	Closed-form[f]
Cauchy	Closed-form[a]	Closed-form[g]	Closed-form[g]	Closed-form[g]	Closed-form[g]	Closed-form[g]

[a] van Genuchten (1981), [b]Wilson and Miller (1978), [c] Wexler (1992); Wang and Wu (2009), [d]Yeh (1981), [e] Leij et al. (1991), [f]Domenico and Robbins (1985); Martin-Hayden and Robbins (1997); Sangani and Srinivasan (2021), and [g] this paper

$$C = 0; \quad \forall \quad 0 < x < \infty, \quad -\infty < y < \infty, \quad -\infty < z < \infty, \quad t = 0 \tag{3}$$

The non-source boundary conditions for the semi-infinite groundwater aquifer are given as:

$$\begin{aligned} \lim_{x\to\infty} \frac{\partial C}{\partial x} &= 0; \quad \forall \quad -\infty < y < \infty, \quad -\infty < z < \infty, \quad t > 0 \\ \lim_{y\to\pm\infty} \frac{\partial C}{\partial y} &= 0; \quad \forall \quad 0 < x < \infty, \quad -\infty < z < \infty, \quad t > 0 \\ \lim_{z\to\pm\infty} \frac{\partial C}{\partial z} &= 0; \quad \forall \quad 0 < x < \infty, \quad -\infty < y < \infty, \quad t > 0 \end{aligned} \tag{4}$$

If q is the rate at which a solute mass is injected into the aquifer [g day^{-1}], then the equations for the exponentially decaying flux of point, line, and area sources subject to the Cauchy boundary condition are given as:

$$\begin{aligned} v_x C - v_x \alpha_x \frac{\partial C}{\partial x} &= \begin{cases} q\,\delta(y - Y_c)\delta(z - Z_c)\exp^{-\lambda t}; & \forall\,(x,y,z) \in S \text{ and } t > 0 \\ 0; & \text{otherwise} \end{cases} \\ v_x C - v_x \alpha_x \frac{\partial C}{\partial x} &= \begin{cases} \frac{q}{Y_w}\delta(z - Z_c)\exp^{-\lambda t}; & \forall\,(x,y,z) \in S \text{ and } t > 0 \\ 0; & \text{otherwise} \end{cases} \\ v_x C - v_x \alpha_x \frac{\partial C}{\partial x} &= \begin{cases} \frac{q}{Z_w}\delta(y - Y_c)\exp^{-\lambda t}; & \forall\,(x,y,z) \in S \text{ and } t > 0 \\ 0; & \text{otherwise} \end{cases} \\ v_x C - v_x \alpha_x \frac{\partial C}{\partial x} &= \begin{cases} \frac{q}{Y_w Z_w}\exp^{-\lambda t}; & \forall\,(x,y,z) \in S \text{ and } t > 0 \\ 0; & \text{otherwise} \end{cases} \end{aligned} \tag{5}$$

where X_c, Y_c, and Z_c are the x, y, and z locations of the source center, Y_w and Z_w are the source widths in the y, and z directions [m], respectively, $\delta(y - Y_c)$ and $\delta(z - Z_c)$ are the Dirac-delta functions [m^{-1}] whose inverse is used to represent the infinitesimally small source widths in the y and z directions, respectively, S is the spatial extent of the source zone (see Table 2), and λ is the first-order decay coefficient of the source [day^{-1}].

$\frac{q}{Y_w Z_w}$ has the units of [g m^{-2} day^{-1}] and represents the mass flux per unit area along the x direction, normal to the y-z plane. Similarly, $\frac{q}{Z_w}\delta(y - Y_c)$, $\frac{q}{Y_w}\delta(z - Z_c)$, and $q\,\delta(y - Y_c)\delta(z - Z_c)$ represent mass flux per unit area with the units of [g m^{-2} day^{-1}].

Equation 5 can also be represented as:

$$\begin{aligned} v_x C - v_x \alpha_x \frac{\partial C}{\partial x} &= \begin{cases} \overset{point}{v_x C_0}\,\delta(y - Y_c)\delta(z - Z_c)\exp^{-\lambda t}; & \forall\,(x,y,z) \in S \text{ and } t > 0 \\ 0; & \text{otherwise} \end{cases} \\ v_x C - v_x \alpha_x \frac{\partial C}{\partial x} &= \begin{cases} \overset{y-line}{v_x C_0}\,\delta(z - Z_c)\exp^{-\lambda t}; & \forall\,(x,y,z) \in S \text{ and } t > 0 \\ 0; & \text{otherwise} \end{cases} \\ v_x C - v_x \alpha_x \frac{\partial C}{\partial x} &= \begin{cases} \overset{z-line}{v_x C_0}\,\delta(y - Y_c)\exp^{-\lambda t}; & \forall\,(x,y,z) \in S \text{ and } t > 0 \\ 0; & \text{otherwise} \end{cases} \\ v_x C - v_x \alpha_x \frac{\partial C}{\partial x} &= \begin{cases} \overset{area}{v_x C_0}\exp^{-\lambda t}; & \forall\,(x,y,z) \in S \text{ and } t > 0 \\ 0; & \text{otherwise} \end{cases} \end{aligned} \tag{6}$$

Table 2 Generalized solutions for the exact semi-analytical solution (C_{exa}) and approximate closed-form solutions (C_{app}) for the three-dimensional reactive transport problem given by governing equation Eq. 2, initial condition Eq. 3, non-source boundary conditions Eq. 4, for point, line, and area sources, with Dirichlet (Eq. 7) and Cauchy (Eq. 6) source boundary conditions.

	Source dimensions (S)	Exact (C_{exa})	Approximate (C_{app})
Point	$x = X_c, y = Y_c, z = Z_c$	$\overset{point}{\frac{C_0}{8}} \exp^{-\lambda t} \int_0^t f_x(x,\tau) \overset{point}{f_y}(y,\tau) \overset{point}{f_z}(z,\tau) \frac{d\tau}{\tau}$	$\overset{point}{\frac{C_0}{8}} \exp^{-\lambda t} \phi_x(x,t) \overset{point}{f_y}(y,\mathrm{T}) \overset{point}{f_z}(z,\mathrm{T})$
y-line	$x = X_c, Y_c - \frac{Y_w}{2} < y < Y_c + \frac{Y_w}{2}, z = Z_c$	$\overset{y-line}{\frac{C_0}{8}} \exp^{-\lambda t} \int_0^t f_x(x,\tau) \overset{line}{f_y}(y,\tau) \overset{point}{f_z}(z,\tau) \frac{d\tau}{\tau}$	$\overset{y-line}{\frac{C_0}{8}} \exp^{-\lambda t} \phi_x(x,t) \overset{line}{f_y}(y,\mathrm{T}) \overset{point}{f_z}(z,\mathrm{T})$
z-line	$x = X_c, y = Y_c, Z_c - \frac{Z_w}{2} < z < Z_c + \frac{Z_w}{2}$	$\overset{z-line}{\frac{C_0}{8}} \exp^{-\lambda t} \int_0^t f_x(x,\tau) \overset{point}{f_y}(y,\tau) \overset{line}{f_z}(z,\tau) \frac{d\tau}{\tau}$	$\overset{z-line}{\frac{C_0}{8}} \exp^{-\lambda t} \phi_x(x,t) \overset{point}{f_y}(y,\mathrm{T}) \overset{line}{f_z}(z,\mathrm{T})$
Area	$x = X_c, Y_c - \frac{Y_w}{2} < y < Y_c + \frac{Y_w}{2}, Z_c - \frac{Z_w}{2} < z < Z_c + \frac{Z_w}{2}$	$\overset{area}{\frac{C_0}{8}} \exp^{-\lambda t} \int_0^t f_x(x,\tau) \overset{line}{f_y}(y,\tau) \overset{line}{f_z}(z,\tau) \frac{d\tau}{\tau}$	$\overset{area}{\frac{C_0}{8}} \exp^{-\lambda t} \phi_x(x,t) \overset{line}{f_y}(y,\mathrm{T}) \overset{line}{f_z}(z,\mathrm{T})$

where $\overset{area}{C_0} = \frac{q}{v_x Y_w Z_w}$, $\overset{y-line}{C_0} = \frac{q}{v_x Z_w}$, $\overset{z-line}{C_0} = \frac{q}{v_x Y_w}$, and $\overset{point}{C_0} = \frac{q}{v_x}$. The units of $\overset{area}{C_0}$ are [mg L^{-1}], while the units of $\overset{y-line}{C_0}$ and $\overset{z-line}{C_0}$ are [mg L^{-1} m], and the units of $\overset{point}{C_0}$ are [mg L^{-1} m^2].

The equations for the Dirichlet source boundary condition can be obtained from Eq. 6 by forcing the dispersion terms of the source flux as 0, i.e., $v_x \alpha_x \frac{\partial C}{\partial x} = 0$. This is given as:

$$
\begin{aligned}
C &= \begin{cases} \overset{point}{C_0}\, \delta(y - Y_c)\delta(z - Z_c) \exp^{-\lambda t}; & \forall\, (x, y, z) \in S \text{ and } t > 0 \\ 0 & \text{otherwise} \end{cases} \\
C &= \begin{cases} \overset{y-line}{C_0}\, \delta(z - Z_c) \exp^{-\lambda t}; & \forall\, (x, y, z) \in S \text{ and } t > 0 \\ 0 & \text{otherwise} \end{cases} \\
C &= \begin{cases} \overset{z-line}{C_0}\, \delta(y - Y_c) \exp^{-\lambda t}; & \forall\, (x, y, z) \in S \text{ and } t > 0 \\ 0 & \text{otherwise} \end{cases} \\
C &= \begin{cases} \overset{area}{C_0} \exp^{-\lambda t}; & \forall\, (x, y, z) \in S \text{ and } t > 0 \\ 0 & \text{otherwise} \end{cases}
\end{aligned}
\tag{7}
$$

The generalized exact semi-analytical solutions (C_{exa}) for both the Dirichlet and Cauchy boundary conditions are presented in Table 2. These were derived using standard Laplace, Fourier, and variable transform techniques (Leij et al. 1991; Wexler 1992). Wang et al. (2011) showed that three-dimensional solutions can also be obtained by integrating the product of one-dimensional advection–dispersion solutions along the x direction (f_x term) with the transverse dispersion solutions (f_y and f_z terms) along the y and z directions.

Note that the $f_x(x, \tau)$ term in Table 2 represents the advective dispersive transport along the x direction and is dimensionless. The $\overset{line}{f_y}(y, \tau)$ and $\overset{line}{f_z}(z, \tau)$ terms account for transverse dispersion of contaminant in a finite-width source dimension along the y and z directions, respectively, and are dimensionless. The transverse dispersion terms $\overset{point}{f_y}(y, \tau)$ and $\overset{point}{f_z}(z, \tau)$ are used when contaminant sources have infinitesimal widths along the y and z directions, respectively, and have the units of [m^{-1}].

$\overset{point}{f_y}(y, \tau)$ and $\overset{point}{f_z}(z, \tau)$ are given as (Wexler 1992):

$$
\begin{aligned}
\overset{point}{f_y}(y, \tau) &= \frac{1}{\sqrt{\pi v_x \alpha_y \tau}} \exp\left[-\frac{(y - Y_c)^2}{4\alpha_y v_x \tau}\right] \\
\overset{point}{f_z}(z, \tau) &= \frac{1}{\sqrt{\pi v_x \alpha_z \tau}} \exp\left[-\frac{(z - Z_c)^2}{4\alpha_z v_x \tau}\right]
\end{aligned}
\tag{8}
$$

$\overset{line}{f_y}(y, \tau)$ and $\overset{line}{f_z}(z, \tau)$ are given as (Wexler 1992):

$$
\begin{aligned}
{}^{line}_{}f_y(y,\tau) &= \operatorname{erf}\left[\frac{y - Y_c + \frac{Y_w}{2}}{2\sqrt{\alpha_y v_x \tau}}\right] - \operatorname{erf}\left[\frac{y - Y_c - \frac{Y_w}{2}}{2\sqrt{\alpha_y v_x \tau}}\right] \\
{}^{line}_{}f_z(z,\tau) &= \operatorname{erf}\left[\frac{z - Z_c + \frac{Z_w}{2}}{2\sqrt{\alpha_z v_x \tau}}\right] - \operatorname{erf}\left[\frac{z - Z_c - \frac{Z_w}{2}}{2\sqrt{\alpha_z v_x \tau}}\right]
\end{aligned}
\tag{9}
$$

2.1 Exact Semi-Analytical Solution

2.1.1 Solution for Cauchy Boundary Condition

The f_x term for the exponentially decaying Cauchy source boundary condition is given as (Leij et al. 1991):

$$
\begin{aligned}
f_x(x,\tau) = {} & \frac{2v_x\tau}{\sqrt{\pi\alpha_x v_x \tau}} \exp\left[\frac{x - X_c}{2\alpha_x}\right] \exp\left[\frac{-v_x\tau}{4\alpha_x} - \frac{(x - X_c)^2}{4\alpha_x v_x \tau} - (k - \lambda)\tau\right] \\
& - \frac{v_x}{\alpha_x\sqrt{\tau}} \exp\left[\frac{x - X_c}{\alpha_x} - (k - \lambda)\tau\right] \operatorname{erfc}\left[\frac{x - X_c + v_x\tau}{2\sqrt{\alpha_x v_x \tau}}\right]
\end{aligned}
\tag{10}
$$

2.1.2 Solution for Dirichlet Boundary Condition

The f_x term for the exponentially decaying Dirichlet source boundary condition is given as (Wexler 1992):

$$
f_x(x,\tau) = \frac{x - X_c}{\sqrt{\pi\alpha_x v_x \tau}} \exp\left[\frac{x - X_c}{2\alpha_x}\right] \exp\left[\frac{-v_x\tau}{4\alpha_x} - \frac{(x - X_c)^2}{4\alpha_x v_x \tau} - (k - \lambda)\tau\right] \tag{11}
$$

2.2 Approximate Closed-Form Solution

The approximate closed-form solution (C_{app}) is obtained by substituting $\tau = \mathrm{T}$ in the f_y and f_z terms of the exact semi-analytical solution. This decouples the transverse dispersion terms f_y and f_z from the variable of integration τ. The remaining integral with only the f_x term can be integrated analytically to yield a closed-form analytical solution. This is expressed as:

$$
\int_0^t f_x(x,\tau) f_y(y,\mathrm{T}) f_z(z,\mathrm{T}) \frac{d\tau}{\tau} = f_y(y,\mathrm{T}) f_z(z,\mathrm{T}) \int_0^t f_x(x,\tau) \frac{d\tau}{\tau} = \phi(x,t) f_y(y,\mathrm{T}) f_z(z,\mathrm{T}) \tag{12}
$$

where $\phi(x,t)$ is the solution to the one-dimensional advective–dispersive transport along the x direction. $\phi(x,t)$ is dimensionless.

T is the characteristic average residence time at a given plume location and represents a solute particle's average time to disperse in the transverse direction (Sangani and Srinivasan 2021). The improved (S &S) approximation for T_{app} is given as (Sangani and Srinivasan 2021):

$$T_{app} = \frac{x - X_c}{v_x}\left[1 + \left(\frac{x - X_c}{v_x t}\right)^n\right]^{\frac{-1}{n}} \tag{13}$$

where n is the shape or curvature parameter is given as:

$$n = \left[\frac{v_x t}{\alpha_x}\right]^{\beta} \tag{14}$$

where β is the empirical exponent parameter with a value of 0.25 [-]. The accuracy of the improved approximation is relatively insensitive to the parameter β within the range of $0.2 < \beta < 0.3$ (Sangani and Srinivasan 2021). Note that, in the absence of longitudinal dispersion ($\alpha_x = 0$), the approximate solutions will be identical to the exact solutions (Srinivasan et al. 2007).

2.2.1 Solution for Cauchy Boundary Condition

When $k \geq \lambda - \frac{v_x}{4\alpha_x}$, the ϕ_x term is given as (van Genuchten 1982):

$$\begin{aligned}\phi_x(x,t) = {} & \frac{2}{1 + \sqrt{1 + \frac{4\alpha_x(k-\lambda)}{v_x}}} \exp\left[\frac{x - X_c}{2\alpha_x}\left(1 - \sqrt{1 + \frac{4(k-\lambda)\alpha_x}{v_x}}\right)\right] \\ & \operatorname{erfc}\left[\frac{x - X_c - v_x t\sqrt{1 + \frac{4(k-\lambda)\alpha_x}{v_x}}}{2\sqrt{\alpha_x v_x t}}\right] \\ & + \frac{2}{1 - \sqrt{1 + \frac{4(k-\lambda)\alpha_x}{v_x}}} \exp\left[\frac{x - X_c}{2\alpha_x}\left(1 + \sqrt{1 + \frac{4(k-\lambda)\alpha_x}{v_x}}\right)\right] \\ & \operatorname{erfc}\left[\frac{x - X_c + v_x t\sqrt{1 + \frac{4(k-\lambda)\alpha_x}{v_x}}}{2\sqrt{\alpha_x v_x t}}\right] \\ & + \frac{v_x}{\alpha_x(k-\lambda)} \exp\left[\frac{x - X_c}{\alpha_x} - kt\right] \operatorname{erfc}\left[\frac{x - X_c + v_x t}{2\sqrt{\alpha_x v_x t}}\right]\end{aligned} \tag{15}$$

When $k = \lambda$, the ϕ_x term is given as (van Genuchten 1982):

$$\phi_x(x,t) = 1 - \exp^{-(k+\lambda)t}\left\{2 - \text{erfc}\left[\frac{x - X_1 - v_x t}{2\sqrt{\alpha_x v_x t}}\right] - 2\sqrt{\frac{v_x t}{\pi\alpha_x}}\exp\left[\frac{-(x - X_1 - v_x t)^2}{4\alpha_x v_x t}\right] + \left[1 + \frac{x - X_1}{\alpha_x} + \frac{v_x t}{\alpha_x}\right]\exp\left[\frac{x - X_1}{\alpha_x}\right]\text{erfc}\left[\frac{x - X_1 + v_x t}{2\sqrt{\alpha_x v_x t}}\right]\right\} \tag{16}$$

When $k < \lambda - \frac{v_x}{4\alpha_x}$, the terms within the square root in Eq. 15 become negative, resulting in complex numbers. However, the different complex number terms cancel out (Srinivasan and Clement 2008a), yielding a real-valued final solution given as (see supplementary section S1):

$$\begin{aligned}\phi_x(x,t) = &\frac{2}{1 + \left|1 + \frac{4(k-\lambda)\alpha_x}{v_x}\right|}\exp\left[\frac{x - X_1}{2\alpha_x}\right]\left[\omega_r - \omega_i\sqrt{\left|1 + \frac{4(k-\lambda)\alpha_x}{v_x}\right|}\right] \\ &\cos\left[\frac{x - X_1}{2\alpha_x}\sqrt{\left|1 + \frac{4(k-\lambda)\alpha_x}{v_x}\right|}\right] \\ &- \frac{2}{1 + \left|1 + \frac{4(k-\lambda)\alpha_x}{v_x}\right|}\exp\left[\frac{x - X_1}{2\alpha_x}\right]\left[\omega_r\sqrt{\left|1 + \frac{4(k-\lambda)\alpha_x}{v_x}\right|} + \omega_i\right] \\ &\sin\left[\frac{x - X_1}{2\alpha_x}\sqrt{\left|1 + \frac{4(k-\lambda)\alpha_x}{v_x}\right|}\right] \\ &+ \frac{v_x}{2\alpha_x(k-\lambda)}\exp\left[\frac{x - X_1}{\alpha_x} - kt\right]\text{erfc}\left[\frac{x - X_1 + v_x t}{2\sqrt{\alpha_x v_x t}}\right]\end{aligned} \tag{17}$$

where ω_r and ω_i are the real and imaginary parts of the error function given as:

$$\text{erfc}\left[\frac{x - X_c + v_x t\sqrt{1 + \frac{4(k-\lambda)\alpha_x}{v_x}}}{2\sqrt{\alpha_x v_x t}}\right] = \omega_r + i\,\omega_i \tag{18}$$

where $i = \sqrt{-1}$.

2.2.2 Solution for Dirichlet Boundary Condition

When $k \geq \lambda - \frac{v_x}{4\alpha_x}$, the ϕ_x term (dimensionless) is given as (Martin-Hayden and Robbins 1997):

$$\phi_x(x,t) = \exp\left[\frac{x-X_c}{2\alpha_x}\left(1-\sqrt{1+\frac{4(k-\lambda)\alpha_x}{v_x}}\right)\right]\operatorname{erfc}\left[\frac{x-X_c-v_x t\sqrt{1+\frac{4(k-\lambda)\alpha_x}{v_x}}}{2\sqrt{\alpha_x v_x t}}\right] + \exp\left[\frac{x-X_c}{2\alpha_x}\left(1+\sqrt{1+\frac{4(k-\lambda)\alpha_x}{v_x}}\right)\right]\operatorname{erfc}\left[\frac{x-X_c+v_x t\sqrt{1+\frac{4(k-\lambda)\alpha_x}{v_x}}}{2\sqrt{\alpha_x v_x t}}\right] \tag{19}$$

When $k < \lambda - \frac{v_x}{4\alpha_x}$, the terms within the square root become negative, resulting in complex numbers. However, the different complex number terms cancel out (Srinivasan and Clement 2008a), yielding a real-valued final solution given as (see supplementary section S2):

$$\phi_x(x,t) = 2\exp\left[\frac{x-X_c}{2\alpha_x}\right]\omega_r \cos\left[\frac{x-X_c}{2\alpha_x}\sqrt{\left|1+\frac{4(k-\lambda)\alpha_x}{v_x}\right|}\right] - 2\exp\left[\frac{x-X_c}{2\alpha_x}\right]\omega_i \sin\left[\frac{x-X_c}{2\alpha_x}\sqrt{\left|1+\frac{4(k-\lambda)\alpha_x}{v_x}\right|}\right] \tag{20}$$

where ω_i and ω_r are given by Eq. 18.

3 Extended Solutions

3.1 Adsorption

The effect of linear equilibrium sorption on the fate and transport of solutes in groundwater can be modeled using retardation factor R [-]. The governing equation (Eq. 2) for the case when decay occurs only in the liquid phase can be represented as:

$$R\frac{\partial C}{\partial t} = -v_x\frac{\partial C}{\partial x} + v_x\alpha_x\frac{\partial^2 C}{\partial x^2} + v_x\alpha_y\frac{\partial^2 C}{\partial y^2} + v_x\alpha_z\frac{\partial^2 C}{\partial z^2} - kC \tag{21}$$

The exact semi-analytical solutions and the approximate closed-form analytical solutions in the presence of retardation factor R are computed by dividing the advection velocity v_x and decay coefficient k by R. The solutions for the point, line, and area source boundaries are then computed using the modified v_x and k parameters. The source decay parameter λ remains unaffected in the presence of the retardation factor. If decay occurs in both the liquid and the adsorbed solid phases, only the advection velocity v_x is divided by R.

3.2 Pulse Source Boundary

If the source boundary is a pulse, where the boundary condition is applied only for a finite amount of time, the domain ranges for the Dirichlet and Cauchy source boundary condition equations (Eqs. 7, 6) are modified as $\forall\,(x, y, z) \in S$ and $0 < t < t_p$. Note that t_p represents the duration of the pulse source input [days].

For the case, when $t < t_p$, the solution for the pulse boundary is the same as before (Sec: 2). However, when $t > t_p$, the solution for the pulse boundary is modified as follows.

3.2.1 Exact Semi-Analytical Solution

The general expression for the exact semi-analytical solution for point, line, or area pulse source boundary condition is given as:

$$C_{\text{exa}}(x, y, z, t, t_p) = \frac{C_0}{8} \exp^{-\lambda t} \int_{t-t_p}^{t} f_x(x, \tau)\, f_y(y, \tau)\, f_z(z, \tau) d\tau \tag{22}$$

where $f_x(x, \tau)$, $f_z(y, \tau)$, and $f_z(z, \tau)$ are given in Eqs. 10, 11, 8, and 9 for the point, line, and area sources (refer to Table 2 for solutions to different sources).

3.2.2 Approximate Closed-Form Analytical Solution

The general expression for the approximate closed-form analytical solution for point, line, or area pulse source boundary condition is given as:

$$C_{\text{app}}(x, y, z, t, t_p) = \frac{C_0}{8} \exp^{-\lambda t} \left[\phi_x(x, t) - \phi_x(x, t - t_p)\right] f_y(y, \mathrm{T})\, f_z(z, \mathrm{T}) \tag{23}$$

where $\phi_x(x, t)$, $f_z(y, \mathrm{T})$, and $f_z(z, \mathrm{T})$ are given in Eqs. 15, 16, 17, 19, 20, 8, and 9 for the point, line, and area sources (refer to Table 2 for solutions to different sources).

3.3 Two-Dimensional Solutions

Forcing $f_z(z, \tau) = 2$ will provide solutions to two-dimensional problems in the x-y plane, while forcing $f_y(y, \tau) = 2$ will result in solutions to two-dimensional problems in the x-z plane. These solutions represent advection–dispersion–reaction transport. However, forcing $f_x(x, \tau) = 2$ results in a purely diffusive two-dimensional solution along the y-z plane since advection is along the x direction. Two-dimensional purely diffusive transport problems only have exact semi-analytical solutions. Closed-form approximate solutions are not valid for purely diffusive two-dimensional transport problems. This is because the characteristic residence time is not defined as $v_x \to 0$.

3.4 One-Dimensional Solutions

The solutions for one-dimensional problems along the x direction with both advection and dispersion are readily obtained by forcing $f_y(y, \tau) = 2$ and $f_z(z, \tau) = 2$. This results in an exact closed-form analytical solution given by $\phi(x)$. Forcing $f_x(x, \tau) = 2$, and making either $f_y(y, \tau) = 2$ or $f_z(z, \tau) = 2$ will provide closed-form exact analytical solutions along

the y or z directions, respectively. This corresponds to a purely diffusive one-dimensional transport, and its solutions are given in supplementary section S3 (van Genuchten 1981; Srinivasan and Clement 2008b).

4 Solution Implementation

The exact semi-analytical and the approximate closed-form analytical solutions for point, line, and area sources under Dirichlet and Cauchy boundary conditions were implemented in a computer program (v-Screen) using MATLAB, the MathWorks Inc., 2021a. The modular computer program has independent functions to calculate C_{exa} and C_{app} solutions. C_{exa} was evaluated using the in-built 'integral' function in MATLAB, which employs a global adaptive quadrature integration technique (Shampine 2008). Since the plume is symmetric about the centerline along the y and z directions, only a quarter of the plume domain is simulated ($x > X_c$, $y > Y_c$, and $z > Z_c$) to improve computational time. The other portions of the plume will simply be a mirror image of these quarter plume. The source code for v-Screen can be obtained from this link: https://github.com/ecohydrologylab/vScreenMatlab/.

While in-built functions were used to evaluate error functions, complementary error functions, and complex error functions, the direct application of these in-built functions in the solution formulation resulted in underflow and overflow errors. Typically, this occurs when computing the product of error function terms (underflow error) with exponential terms (overflow error) (van Genuchten 1985; Srinivasan and Clement 2008b). A logarithmic transformation formulation was employed to overcome the underflow and overflow errors. In this formulation, the error function and exponential terms were first transformed from the linear space to log space. The multiplication operation in the linear space becomes a summation operation in the log space. The sum of the log-transformed terms was then inverse-transformed to the linear space to evaluate the product terms (Srinivasan and Clement 2008b). This logarithmic transformation method significantly reduced underflow and overflow errors.

The exact semi-analytical solutions were validated against an explicit finite difference numerical solution (C_{num}) for the point, line, and area source geometries under Dirichlet and Cauchy boundaries (see supplementary section S4 for details of numerical methods). Additionally, the approximate S &S solutions were compared against the exact semi-analytical solutions.

5 Results

Field-scale example problems for point (Yeh 1981), line (Wexler 1992), and area (Domenico and Robbins 1985) sources were considered for these model simulations (see Table 3 for model parameters). While the original example problems had a Dirichlet boundary condition, a Cauchy boundary condition was added to all three example problems. The Cauchy boundary conditions were formulated such that the source flux of the Dirichlet and Cauchy boundary conditions is equal in the absence of longitudinal dispersion. Additionally, sensitivity simulations were performed under higher longitudinal dispersivity values ($10\alpha_x$) to test the performance of the approximate solutions under critical parameter sensitivity conditions (Srinivasan et al. 2007; Sangani and Srinivasan 2021).

Table 3 List of parameters used in the model comparison simulations for point (Yeh 1981), line (Wexler 1992), and area (Domenico and Robbins 1985) source boundary conditions.

Parameter	Symbol	Unit	Point	Line	Area
Longitudinal dispersivity	α_x	[m]	30	21.34	42.58
Transverse dispersivity in y	α_y	[m]	5	4.2672	8.43
Transverse dispersivity in z	α_z	[m]	5	0	0.00642
Velocity	v_x	[m day^{-1}]	0.125	0.432	0.2151
Simulation time	t	[day]	240	1826	5110
Source pulse time	t_p	[day]	240	1826	5110
Plume decay coefficient	k	[day^{-1}]	0	0	0
Source decay coefficient	λ	[day^{-1}]	0	0	0
Dirichlet boundary condition	C_0	Variable	1	40	850
Cauchy boundary condition	$v_x C_0$	Variable	0.125	17.28	182.8
Source center x-location	X_c	[m]	0	0	0
Source center y-location	Y_c	[m]	10	228	0
Source center z-location	Z_c	[m]	1	0	0
Source y-width	Y_w	[m]	0	70	240
Source z-width	Z_w	[m]	0	0	5

5.1 Characteristic residence Time

The approximate characteristic residence times for the S &S solutions (T_{app}) were computed from Eq. 13. The true characteristic residence times for the exact semi-analytical solutions (T_{exa}) were calculated using the inverse method described in Sangani and Srinivasan (2021). T_{exa} has three features i) initial linear behavior with slope $= v_x^{-1}$, ii) final saturation value of t, and iii) transition behavior between features i) and ii) in the region surrounding the advective front (Sangani and Srinivasan 2021).

Model simulations for the point, line, and area sources under both Dirichlet and Cauchy boundary conditions show that, along the plume centerline, T_{app} captures the three different features of T_{exa} well both within and beyond the advective front (Fig. 1). Parameter sensitivity simulations for α_x show a marginal increase in the errors of T_{app} closer to the source, as observed in Sangani and Srinivasan (2021). As expected, T_{app} errors decrease with decreasing α_x. These simulations show that the characteristic residence time approximation derived originally for a rectangular area source under Dirichlet boundary conditions (Sangani and Srinivasan 2021) is valid for point and line sources under both Dirichlet and Cauchy boundary conditions and area sources under Cauchy boundary conditions.

5.2 Point Source Boundary Condition

Along the plume centerline, the concentrations predicted by the exact semi-analytical solution (C_{exa}) reproduce the results of the numerical solution (C_{num}) under both Dirichlet and Cauchy boundary conditions (Fig. 2 a, d). The S &S approximate solution (C_{app}) matches well with C_{exa}, especially at plume regions beyond the advective front

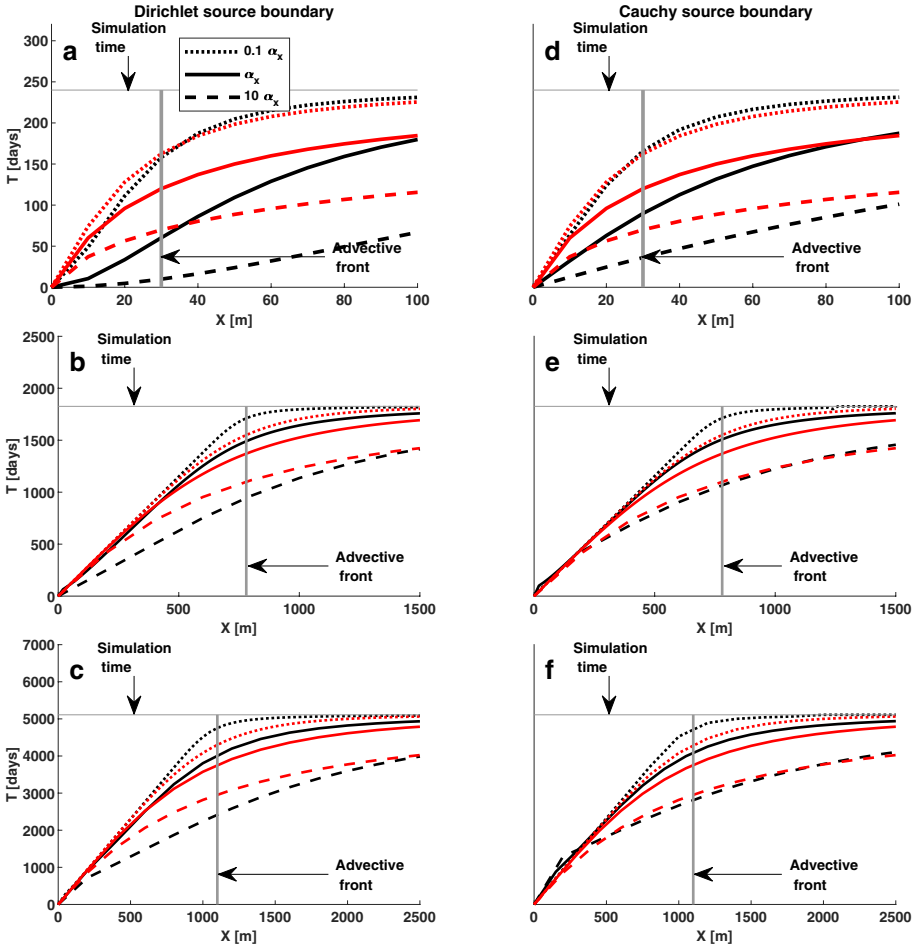

Fig. 1 Variation of the characteristic average residence times of the exact (T_{exa} *black*) and approximate (T_{app} *red*) solutions along the plume centerline for point (**a** and **d**), line (**b**, and **e**), and area (**c** and **f**) sources. The left column (**a**, **b**, and **c**) corresponds to the Dirichlet boundary condition, and the right column (**d**, **e**, and **f**) corresponds to the Cauchy boundary condition. T_{exa} and T_{app} are also plotted for 0.1 α_x (*dotted line*), α_x (*solid line*), and 10α_x (*dashed line*). Model parameters are given in Table 3.

(gray vertical lines). Within the advective front and at plume regions close to the source, C_{app} introduces some errors. These errors are lower under smaller α_x and larger under higher α_x.

Along the y-transect, C_{exa} reproduces the results of C_{num} under both Dirichlet and Cauchy boundary conditions (Fig. 2 b, c, e, and f). As expected, the accuracy of C_{app} is higher beyond the advective front, where it matches well with C_{exa} (Fig. 2 c, and f). However, under higher α_x values, C_{app} introduces some errors within the advective front at plume regions close to the source (Fig. 2 b, and e). This is because the characteristic residence time formulation in the S &S approximation only accounts for longitudinal dispersion effects and ignores transverse dispersion (Sangani and Srinivasan 2021).

The concentration contour plots in the x-y plane show that C_{app} matches with C_{exa} under Dirichlet and Cauchy source boundary conditions (Fig. 3). Even under critical

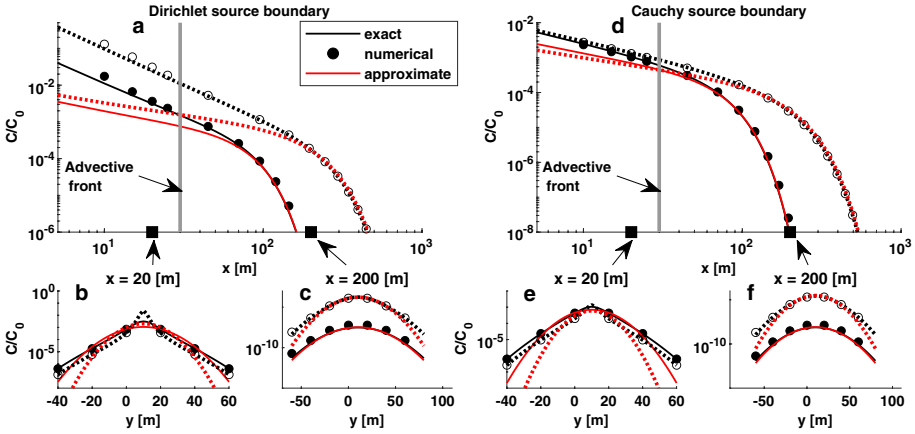

Fig. 2 Comparison of the plume centerline (y = 10 [m], z = 1 [m]) concentration profiles between the exact semi-analytical (C_{app} *black*), numerical (C_{num} *circles*), and the S &S approximate (C_{app} *red*) solutions for the three-dimensional point source example problem with **a** Dirichlet and **d** Cauchy boundary conditions. The concentration profiles along the y-transects within the advective front (x = 20 [m], and z = 1 [m]) **b**, and **e** and beyond the advective front (x = 200 [m], z = 1 [m]) **c**, and **f** are highlighted. Solid lines and filled circles represent base case α_x, while dashed lines and open circles represent parameter sensitivity simulations for $10\alpha_x$. Gray vertical bars indicate the location of the advective front. Model parameters are taken from Yeh (1981) and are summarized in Table 3.

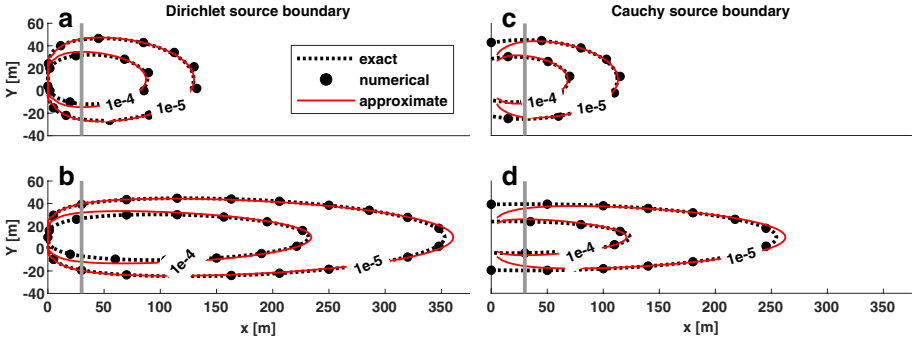

Fig. 3 Comparison of the concentration contours between the exact semi-analytical (C_{exa} *black dashed line*), numerical (C_{num} *black circles*), and the S &S approximate (C_{app} *red solid line*) solutions along the x–y plane (z = 1 [m]) for the three-dimensional point source example problem with Dirichlet (**a**, and **b**) and Cauchy (**c**, and **d**) boundary conditions. **b** and **d** represent parameter sensitivity simulations for $10\alpha_x$. *Gray vertical bars* indicate the location of the advective front. Model parameters are taken from Yeh (1981) and are summarized in Table 3.

parameter conditions ($10\alpha_x$), C_{app} matches well with C_{exa} over large sections of the plume (Fig. 3 b, and d). Similar behavior is also observed in the contour plots in the y-z plane (Fig. S1). These simulations validate the single-integral exact semi-analytical solutions for point source geometry under both Dirichlet and Cauchy boundary conditions. Additionally, these simulations demonstrate that the closed-form S &S approximate solution for the point source geometry matches the exact solution over large sections of the

plume. Under high longitudinal dispersivity values and at plume regions close to the source, the S &S approximate solution shows some discrepancies.

5.3 Line Source Boundary Condition

The line source example problem is a two-dimensional contaminant transport problem in the x-y plane. Since $\alpha_z = 0$, the f_z term in the solution will equals 2. The plume centerline concentrations for the line source example problem show that C_{exa} reproduces the results of C_{num} under both Dirichlet and Cauchy boundary conditions (Fig. 4 a and d). Additionally, C_{app} performs well both within and beyond the advective front. Similar results can be observed in the y-transect plots (Fig. 4 b, c, e, and f).

The x-y contour plots for the line source boundary show that C_{exa} matches C_{num} under both Dirichlet and Cauchy source boundary conditions (Fig. 5 a, and c). C_{app} closely matches C_{exa} even under critical parameter ($10\alpha_x$) conditions (Fig. 5 b, and d). As expected, at regions close to the source and away from the centerline, C_{app} introduces some errors. Overall, C_{app} performs reasonably well over large sections of the plume and closely matches the exact semi-analytical solution.

5.4 Area Source Boundary Condition

Plume centerline simulations for the rectangular area source example problem show that C_{exa} matches C_{num} under both Dirichlet and Cauchy boundaries (Fig. 6 a, and d). While the accuracy of C_{app} for Dirichlet source boundary with an area source has been previously characterized (Srinivasan et al. 2007; Sangani and Srinivasan 2021), its performance for a Cauchy boundary has not been characterized. Along the centerline, C_{app} also closely

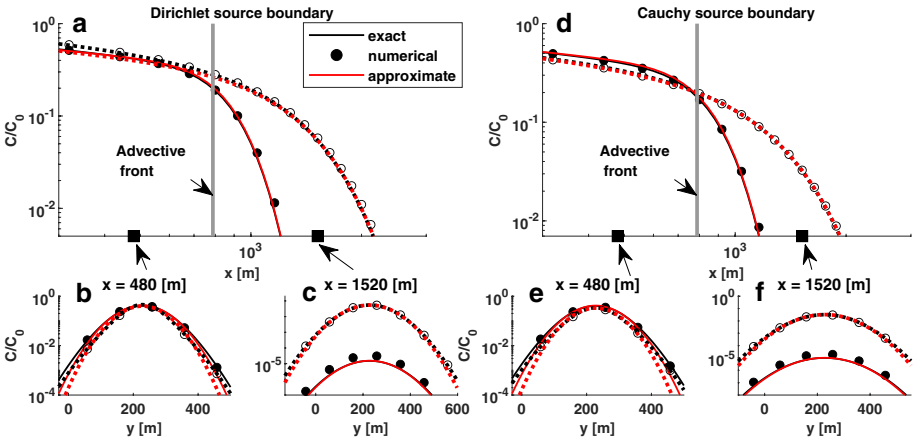

Fig. 4 Comparison of the plume centerline (y = 228 [m]) concentration profiles between the exact semi-analytical (C_{exa} *black*), numerical (C_{num} *circles*), and the S &S approximate (C_{app} *red*) solutions for the two-dimensional line source example problem with **a** Dirichlet and **d** Cauchy boundary conditions. The concentration profiles along the y-transects within the advective front (x = 480 [m]) (**b**, and **e**) and beyond the advective front (x = 1520 [m]) (**c**, and **f**) are highlighted. Solid lines and filled circles represent base case α_x, while *dashed lines* and *open circles* represent parameter sensitivity simulations for $10\alpha_x$. *Gray vertical bars* indicate the location of the advective front. Model parameters are taken from Wexler (1992) and are summarized in Table 3.

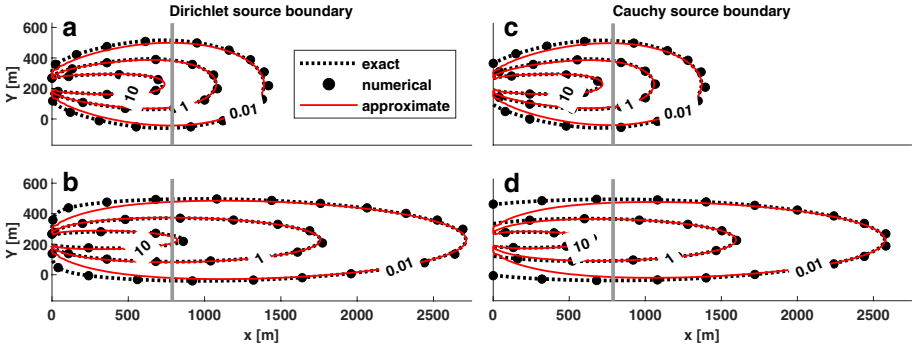

Fig. 5 Comparison of the concentration contours between the exact semi-analytical (C_{exa} black dashed line), numerical (C_{num} circles), and the S &S approximate (C_{app} red solid line) solutions along the x-y plane for the two-dimensional line source example problem with Dirichlet (**a**, and **b**) and Cauchy (**c**, and **d**) boundary conditions. **b** and **d** represent parameter sensitivity simulations for $10\alpha_x$. Gray vertical bars indicate the location of the advective front. Model parameters are taken from Wexler (1992) and are summarized in Table 3.

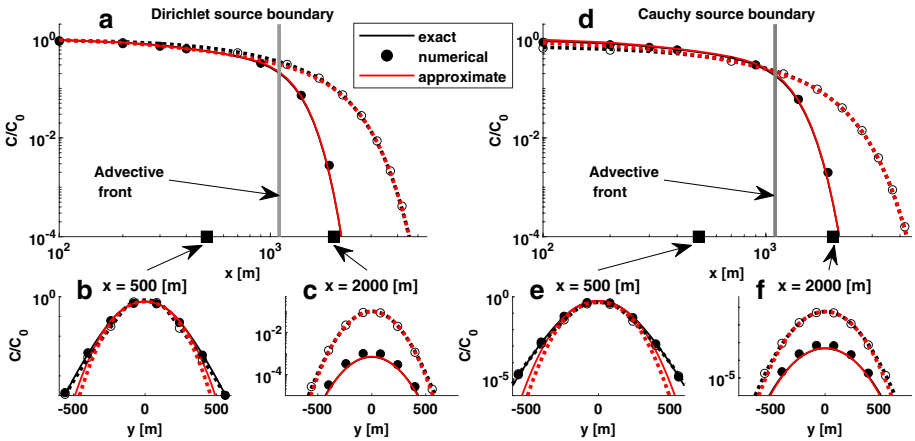

Fig. 6 Comparison of the plume centerline (y = 0 [m], z = 0 [m]) concentration profiles between the exact semi-analytical (C_{exa} *black*), numerical (C_{num} *circles*), and the S &S approximate (C_{app} *red*) solutions for the three-dimensional area source example problem with **a** Dirichlet and **d** Cauchy boundary conditions. The concentration profiles along the y-transects within the advective front (x = 500 [m], and z = 0 [m]) (**b**, and **e**) and beyond the advective front (x = 2000 [m], and z = 0 [m]) (**c**, and **f**) are highlighted. Solid lines represent base case α_x, and *dashed lines* represent parameter sensitivity simulations for $10\alpha_x$. *Gray vertical bars* indicate the location of the advective front. Model parameters are taken from Domenico and Robbins (1985) and are summarized in Table 3.

matches the exact solution. The y-transect plots show that C_{app} performs well both within (Fig. 6 b, and e) and beyond (Fig. 6 c, and f) the advective front.

Contour plots on the x-y plane for the area source boundary show that C_{exa} reproduces the results of C_{num} under both Dirichlet and Cauchy source boundary conditions (Fig. 7 a, and c). Similar to the point and line source example problems, errors in C_{app} marginally increase under higher longitudinal dispersivity values ($10\alpha_x$), especially in regions close to the source

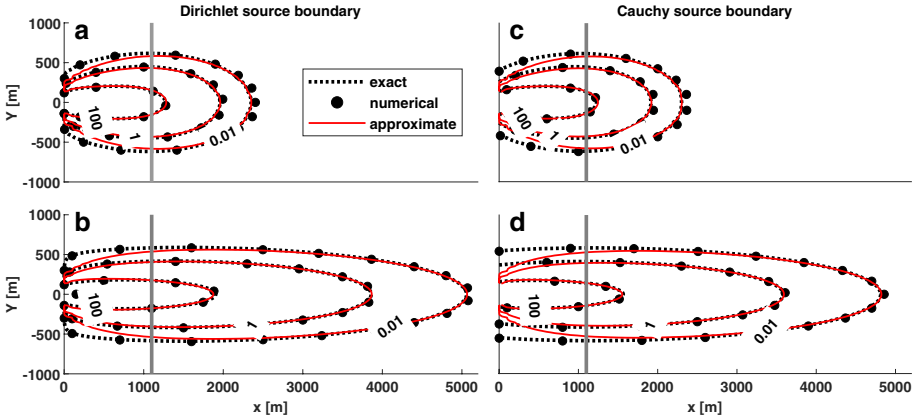

Fig. 7 Comparison of the concentration contours between the exact semi-analytical (C_{exa} *black dashed line*), numerical (C_{num} *circles*), and S &S approximate (C_{app} red solid line) solutions along the x–y plane (z = 0 [m]) for the three-dimensional area source example problem with Dirichlet (**a**, and **b**) and Cauchy (**c**, and **d**) boundary conditions. **b** and **d** represent parameter sensitivity simulations for $10\alpha_x$. *Gray vertical bars* indicate the location of the advective front. Model parameters are taken from Domenico and Robbins (1985) and are summarized in Table 3.

(Fig. 7 b, and d). Beyond the advective front, the C_{app} accurately estimates the plume concentrations. Similar results are observed for concentration contours along the y-z plane (Fig. S2).

5.5 Extended Solutions: Pulse Source and Decay

Using the principle of linear superposition (Eqs. 22 and 23), plume concentrations were obtained for the area source example problem given in Domenico and Robbins (1985) (Table 3) with a modified pulse source boundary condition. The pulse time t_p was set to 510 [days]. Model simulations show that the C_{exa} contours exactly match with C_{num}, and C_{app} closely matches C_{exa} both within and beyond the advective front (Fig. S3).

Model comparison simulations performed so far only included time-invariant source boundary conditions (constant source concentration or constant source flux) for a conservative source. To validate the C_{exa} solution and assess the performance of C_{app} under time-varying (exponentially decaying) source boundary conditions and contaminant plume decay, model simulations were performed using a field-scale, area-source example problem from Paladino et al. (2018). The parameters for this problem are similar to the original Domenico example problem (Domenico and Robbins 1985) with the following modifications i) $\lambda = 0.008$ [day^{-1}], and ii) $k = 0.001$ [day^{-1}] (Table 3). These simulation results show an exact match between C_{exa} and C_{num}, validating the analytical solutions. C_{app} closely matches C_{exa} showing that the derivations under complex number conditions (Eqs. 2017) are valid under both Dirichlet and Cauchy boundary conditions (Fig. S4).

6 Discussion

6.1 Range of Parameters and Domain Conditions

The simulations performed in Sec. 5 only compared the exact and approximate solutions for a limited set of three example problems (Table 3) under parameter sensitivity values to longitudinal dispersivity. However, groundwater transport problems have a wide range of parameter values (Gelhar et al. 1992; Schulze-Makuch 2005) and domain conditions spanning several orders of magnitude in spatiotemporal scales ranging from laboratory experiments to field-scale problems. Previous studies have shown that the longitudinal and transverse dispersivity values increase (Gelhar et al. 1992; Schulze-Makuch 2005) with increasing scale (plume lengths). Based on data from 109 studies, the scaling behavior of longitudinal dispersivity with plume length (ranging from 1 [m] to 100,000 [m]) has been characterized as a power-law relationship (Neuman 1990; Xu and Eckstein 1995; Schulze-Makuch 2005). Some studies suggest a 1 [km] upper bound for longitudinal dispersivity values (Xu and Eckstein, 1995). However, studies with more extensive data sets do not support an upper bound or asymptotic trend for the variation of longitudinal dispersivity with the plume scale (Schulze-Makuch 2005).

Higher longitudinal dispersivity negatively affects the performance of the S &S solution, especially at plume locations closer to the source and away from the plume centerline. To assess the performance of the S &S approximate solution under a range of parameter conditions typically encountered in groundwater contamination scenarios, model simulations were performed considering the entire range of parameters and domain conditions (Table 4). A random (uniformly distributed) combination of parameters and domain values were selected from the observed range of values resulting in 10,000 unique transport problem simulations for each of the six (three source domains with two boundary conditions) classes of transport problems resulting in a total of 60,000 unique transport problem simulations. The maximum value for the plume and source decay coefficient was set assuming a half-life of one year (365 [days]). The domain ranges for these 60,000 simulations are $0 < t < 10,000$ [days], $0 < x - X_c < 10,000$ [m], $0 < y - Y_c < 5,000$ [m], and $0 < z - Z_c < 500$ [m].

Table 4 The observed ranges of parameter values for modeling three-dimensional contaminant transport in groundwater (Gelhar et al. 1992).

Parameter	Symbol	Unit	Range
Longitudinal dispersivity	α_x	[m]	0.43–910
Transverse dispersivity in y	α_y	[m]	0.018–52
Transverse dispersivity in z	α_z	[m]	0.0015–0.1
Velocity	v_x	[m day^{-1}]	0.03–29
Simulation time	t	[day]	1–10,000
Plume decay coefficient	k	[day^{-1}]	0-0.002
Source decay coefficient	λ	[day^{-1}]	0-0.002
Dirichlet: C	C_0	[mg L^{-1}]	variable
Cauchy: $v_x C - v_x \alpha_x \frac{\partial C}{\partial x}$	$v_x C_0$	[m day^{-1} mg L^{-1}]	variable
Source y-width (y-line/area)	Y_w	[m]	1–1000
Source z-width (z-line/area)	Z_w	[m]	1–100

The characteristic times predicted by the S &S approximate solutions (T_{app}) were compared with the exact semi-analytical solution (T_{exa}) for the 60,000 unique transport simulations for plume regions beyond the advective front (Fig. S5). These results show that T_{app} matches well with T_{exa} for the three (point, line, and area) sources and two (Dirichlet and Cauchy) boundary conditions (Fig. S5). Existing screening tools use the closed-form Domenico approximation to represent the characteristic time T_{dom} (Newell et al. 1996; Aziz et al. 2000; Neville 2005; Burnell et al. 2012; Rios et al. 2013; Funk et al. 2017). T_{dom} is given as (Domenico and Robbins 1985; Sangani and Srinivasan 2021):

$$T_{dom} = \frac{x - X_c}{v_x} \tag{24}$$

Comparing T_{dom} with T_{exa} for the 60,000 simulations, the improvement in the S &S approximation becomes apparent (Fig. S5). Beyond the advective front, T_{dom} overestimates the characteristic residence time and incorrectly models T to be higher than the model simulation time (Srinivasan et al. 2007; Sangani and Srinivasan 2021).

The improvement in T is also reflected in the one-to-one concentration predictions, where C_{app} matches well with the C_{exa} over 15 orders of magnitude for the 60,000 unique simulations (Fig. 8). As expected, due to its poor approximation of T, plume concentrations predicted by the Domenico solution (C_{dom}) perform very poorly (Fig. 8). While

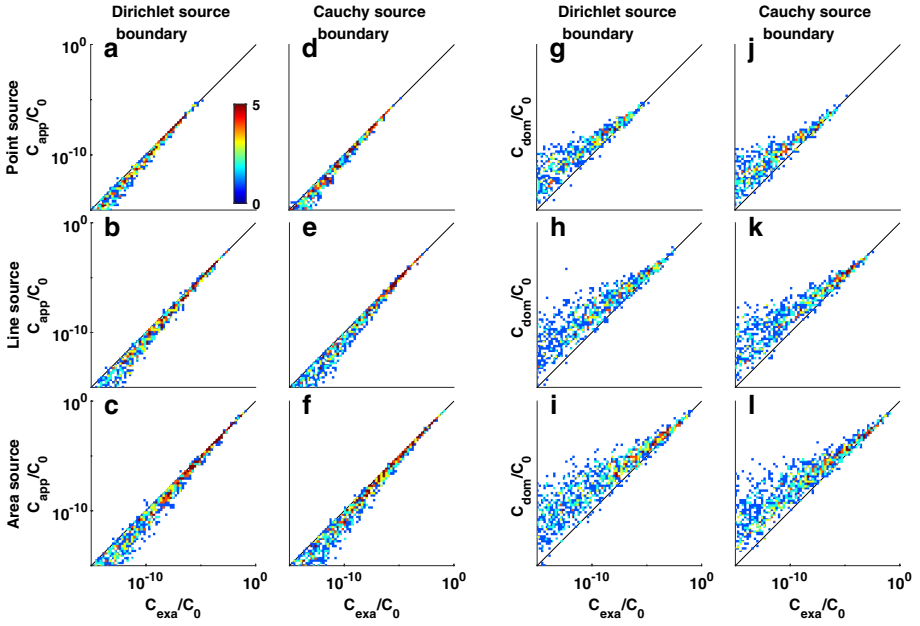

Fig. 8 One-to-one comparison of the normalized plume concentrations of the exact semi-analytical solution (C_{exa}/C_0) with the S &S approximate (C_{app}/C_0) and the Domenico approximate (C_{dom}/C_0) solutions for Dirichlet and Cauchy boundary conditions. Each subplot represents data from 10,000 unique contaminant transport problems sampled from a uniform distribution of parameter ranges and simulation domains (see Table 4). Results are shown for plume regions beyond the advective front. Black diagonal lines represent a 1:1 slope.

Table 5 Summary of relative computing times of different solutions to estimate plume concentrations. Estimates were made for 10,000 individual computations of concentrations on a laptop computer (Intel(R) Core i5-8265U CPU@1.6 Hz, 8GB RAM with Microsoft Windows 10 operating system). The computations for the approximate semi-analytical solutions increase under parameter conditions resulting in complex number computations of ϕ_x (Eqs. 17 and 20).

Solution	Relative computing time $k \geq \lambda - \frac{v_x}{4\alpha_x}$
Approximate	< 1
Semi-analytical	5-6
Numerical	> 10000

C_{dom} significantly overestimates plume concentrations, C_{app} only marginally underestimates plume concentrations beyond the advective front.

6.2 Computational Efficiency

Compared to standard numerical solutions, the exact semi-analytical solutions (C_{exa}) presented in this study are computationally efficient by several orders of magnitude (Table 5). The S &S approximate closed-form analytical solutions (C_{app}) have a 5 times computational advantage over existing exact semi-analytical solutions. When parameter combinations result in complex error function terms, the computational time for C_{app} increases; however, this situation can be improved using efficient algorithms for computing the error function terms.

For example, the S &S solutions take 1 sec to compute the plume concentrations at 1000 locations (typically needed to estimate concentration contours along a given plane) when run using a laptop computer (Intel(R) Core i5-8265U CPU@1.6 Hz, 8GB RAM with Microsoft Windows 10 operating system). However, single-integral exact solutions take 5 seconds for the same simulations. When complex error functions have to be evaluated, the computing times for the S &S approximate solutions marginally increase, while the performance of other solutions remains unchanged. However, this parameter combination occurs relatively infrequently (less than 10% of the time) when solving reactive transport problems.

6.3 Limitations and Future Directions

The semi-analytical solutions presented here are exact solutions that are accurate for all parameter combinations and simulation domain values. However, the closed-form S &S solutions are approximate solutions whose accuracy varies with plume location and transport parameter values. While the S &S approximate solution accurately estimates contaminant concentrations at plume regions beyond the advective front, it introduces some errors at specific plume regions within the advective front. These plume regions are located close to the source and away from the plume centerline. The errors tend to be higher at larger values of longitudinal dispersivities and are such that plume concentrations are always underestimated when compared to exact semi-analytical solutions.

These errors arise because the characteristic average residence times employed by the S &S solutions are based on a centerline approach that ignores the travel time of contaminant particles along the transverse directions (Sangani and Srinivasan 2021). This results in underestimating the characteristic residence time and the corresponding plume concentrations. Adding a transverse correction to the T_{app} formulation can improve the solution accuracy for regions within the advective front. However, determining the functional form of the transverse correction terms and their associated parameters such that they are generic across different source dimensions (point, line, and area) and boundary conditions (Dirichlet, Cauchy) can be challenging.

The solutions presented so far considered only one species of solute. Typically, contaminant transport problems involve degradation products that are also harmful, and their fate and transport need monitoring (Clement 2001; Quezada et al. 2004; Srinivasan and Clement 2008a). The present framework can be extended to obtain solutions for multi-species coupled reactive transport problems as well. Coupling this with modeling multiple interacting source zones using superposition principles will enable the application of the proposed solutions to a broader set of groundwater contaminant transport problems.

7 Summary and Conclusions

This paper presents a library of exact semi-analytical solutions to groundwater transport problems with one-dimensional advection, one-, two-, or three-dimensional dispersion, first-order decay reaction, and linear equilibrium sorption under both Dirichlet and Cauchy boundary conditions. The transport problem can involve contaminant sources having a point, line, or area geometry, with exponentially decaying time-varying source zone concentration or source flux. These semi-analytical solutions can be employed to validate numerical models. However, semi-analytical solutions require numerical evaluation of a definite integral to compute the final plume concentrations. This adversely affects computational time and makes them cumbersome to use in screening studies.

To improve computational efficiency by eliminating the need for numerical integration, closed-form approximate analytical solutions (S &S solutions) were derived for all the exact semi-analytical solutions using the concept of characteristic average residence time. These approximate solutions can accurately predict plume contours over large sections of the plume under a wide range of parameter conditions, making them ideal for use in screening tools. To overcome restrictions on the choice of transport parameters, special expressions for computing plume concentrations were derived to handle error function terms involving complex numbers.

The exact and approximate analytical solutions are extended to solve transport problems with i) linear equilibrium sorption with the option of plume decay happening in both liquid and solid phases, or only in the liquid phase, and ii) pulse source input. These extensions help broaden the application of these solutions to a wide range of practically relevant simplified groundwater contaminant transport problems. The solutions developed in this paper can be readily implemented in screening tools for the rapid assessment of contaminant plume concentrations. Additionally, these computationally efficient solutions facilitate screening-level parameter estimation and multi-scenario analysis studies.

Supplementary Information The online version contains supplementary material available at https://doi.org/10.1007/s11242-022-01828-x.

Acknowledgements The authors thank the editor and the two anonymous reviewers for their insightful comments and suggestions. This research was partly supported by the Center for Industrial Consultancy and Sponsored Research (ICSR), Indian Institute of Technology Madras, grant numbers: CIE1819847NFIGVENT and CE1920364NFSC008930, and Prime Minister's Research Fellowship from the Department of Science and Technology, India, grant number SB22230182CEPMRF008930.

Funding This research was partly supported by the Center for Industrial Consultancy and Sponsored Research (ICSR), Indian Institute of Technology Madras, grant numbers: CIE1819847NFIGVENT and CE1920364NFSC008930, and Prime Minister's Research Fellowship from the Department of Science and Technology, India, grant number SB22230182CEIITMPMRF008930.

Declarations

Conflict of interest The authors declare that they have no conflict of interest.

References

Aziz, C. E., Newell, C. J., Gonzales, J. R., Haas, P. E., Clement, T. P., Sun, Y.: BIOCHLOR Natural Attenuation Decision Support System. User's Manual Version 1.0. US Environmental Protection Agency (2000)

Batu, V., van Genuchten, M.T.: First-and third-type boundary conditions in two-dimensional solute transport modeling. Water Resources Res. **26**(2), 339–350 (1990). https://doi.org/10.1029/WR026i002p00339

Bear, J.: Dynamics of Fluids in Porous Media. Dover pubications Inc., New York, USA (1972)

Burnell, D.K., Lester, B.H., Mercer, J.W.: Improvements and corrections to AT123D code. Groundwater **50**(6), 943–953 (2012). https://doi.org/10.1111/j.1745-6584.2011.00905.x

Chrysikopoulos, C.V.: Three-dimensional analytical models of contaminant transport from nonaqueous phase liquid pool dissolution in saturated subsurface formations. Water Resources Res. **31**(4), 1137–1145 (1995). https://doi.org/10.1029/94WR02780

Cleary, R., Ungs, M.: Analytical Models for Ground-Water Pollution and Hydrology: Princeton university, waterresources program report 78-wr-15, 165 p. Program, Princeton Univ., Princeton, NJ (1978)

Clement, T.P.: Generalized solution to multispecies transport equations coupled with a first-order reaction network. Water Resources Res. **37**(1), 157–163 (2001). https://doi.org/10.1029/2000WR900239

Domenico, P.A., Robbins, G.A.: A new method of contaminant plume analysis. Groundwater **23**(4), 476–485 (1985). https://doi.org/10.1111/j.1745-6584.1985.tb01497.x

Domenico, P.A.: An analytical model for multidimensional transport of a decaying contaminant species. J. Hydrol. **91**(1–2), 49–58 (1987). https://doi.org/10.1016/0022-1694(87)90127-2

Ellsworth, T., Butters, G.: Three-dimensional analytical solutions to the advection-dispersion equation in arbitrary cartesian coordinates. Water Resources Res. **29**(9), 3215–3225 (1993). https://doi.org/10.1029/93WR01293

Funk, S.P., Hnatyshin, D., Alessi, D.S.: HYDROSCAPE: a new versatile software program for evaluating contaminant transport in groundwater. SoftwareX **6**, 261–266 (2017). https://doi.org/10.1016/j.softx.2017.10.001

Gelhar, L. W., Welty, C., Rehfeldt, K. R. A.: Critical review of data on field-scale dispersion in aquifers' by L. W. Gelhar, C. Welty, and K. R. Water Resources Res. **29**(6), 1867–1869 (1992). https://doi.org/10.1029/92WR00607

Guyonnet, D., Neville, C.: Dimensionless analysis of two analytical solutions for 3-D solute transport in groundwater. J. Contamin. Hydrol. **75**(1–2), 141–153 (2004). https://doi.org/10.1016/j.jconhyd.2004.06.004

Karanovic, M., Neville, C.J., Andrews, C.B.: BIOSCREEN-AT: BIOSCREEN with an exact analytical solution. Groundwater **45**(2), 242–245 (2007). https://doi.org/10.1111/j.1745-6584.2006.00296.x

Leij, F.J., Skaggs, T.H., van Genuchten, M.T.: Analytical solutions for solute transport in three-dimensional semi-infinite porous media. Water Resources Res. **27**(10), 2719–2733 (1991). https://doi.org/10.1029/91WR01912

Leij, F.J., Toride, N., Van Genuchten, M.T.: Analytical solutions for non-equilibrium solute transport in three-dimensional porous media. J. Hydrol. **151**(2–4), 193–228 (1993). https://doi.org/10.1016/0022-1694(93)90236-3

Leij, F.J., Priesack, E., Schaap, M.G.: Solute transport modeled with Green's functions with application to persistent solute sources. J. Contamin. Hydrol. **41**(1–2), 155–173 (2000). https://doi.org/10.1016/S0169-7722(99)00062-5

Martin-Hayden, J.M., Robbins, G.A.: Plume distortion and apparent attenuation due to concentration averaging in monitoring wells. Groundwater **35**(2), 339–346 (1997). https://doi.org/10.1111/j.1745-6584.1997.tb00091.x

Neuman, S.P.: Universal scaling of hydraulic conductivities and dispersivities in geologic media. Water Resources Res. **26**(8), 1749–1758 (1990). https://doi.org/10.1029/WR026i008p01749

Neville, C.J.: ATRANS: Analytical Solutions for Three-Dimensional Solute Transport from a Patch Source (Version 2). Papadopulos and Associates Inc, S.S (2005)

Newell, C.J., McLeod, R.K., Gonzales, J.R.: BIOSCREEN: Natural Attenuation Decision Support System. User's Manual Version 1.3. Technical report, United States Environmental Protection Agency (1996)

Ogata, A., Banks, R.B.: A solution of the differential equation of longitudinal dispersion in porous media: fluid movement in earth materials, Technical Report 411 A, US Geological Survey (1961). https://pubs.er.usgs.gov/publication/pp411A

Paladino, O., Moranda, A., Massabò, M., Robbins, G.A.: Analytical solutions of three-dimensional contaminant transport models with exponential source decay. Groundwater **56**(1), 96–108 (2018). https://doi.org/10.1111/gwat.12564

Quezada, C.R., Clement, T.P., Lee, K.-K.: Generalized solution to multi-dimensional multi-species transport equations coupled with a first-order reaction network involving distinct retardation factors. Adv. Water Resources **27**(5), 507–520 (2004). https://doi.org/10.1016/j.advwatres.2004.02.013

Rios, J.F., Ye, M., Wang, L., Lee, P.Z., Davis, H., Hicks, R.: ArcNLET: a GIS-based software to simulate groundwater nitrate load from septic systems to surface water bodies. Comput. Geosci. **52**, 108–116 (2013). https://doi.org/10.1016/j.cageo.2012.10.003

Sagar, B.: Dispersion in three dimensions: approximate analytic solutions. J. Hydraulics Div. **108**(1), 47–62 (1982). https://doi.org/10.1061/JYCEAJ.0005809

Sangani, J., Srinivasan, V.: Improved domenico solution for three-dimensional contaminant transport. J. Contam. Hydrol. **243**, 103897 (2021). https://doi.org/10.1016/j.jconhyd.2021.103897

Schulze-Makuch, D.: Longitudinal dispersivity data and implications for scaling behavior. Groundwater **43**(3), 443–456 (2005). https://doi.org/10.1111/j.1745-6584.2005.0051.x

Shampine, L.: Vectorized adaptive quadrature in MATLAB. J. Comput. Appl. Math. **211**(2), 131–140 (2008). https://doi.org/10.1016/j.cam.2006.11.021

Sim, Y., Chrysikopoulos, C.V.: Analytical solutions for solute transport in saturated porous media with semi-infinite or finite thickness. Adv. Water Resources **22**(5), 507–519 (1999). https://doi.org/10.1016/S0309-1708(98)00027-X

Srinivasan, V., Clement, T.P.: Analytical solutions for sequentially coupled one-dimensional reactive transport problems - Part I: Mathematical derivations. Adv. Water Resources **31**(2), 203–218 (2008). https://doi.org/10.1016/j.advwatres.2007.08.002

Srinivasan, V., Clement, T.P.: Analytical solutions for sequentially coupled one-dimensional reactive transport problems—Part II: special cases, implementation and testing. Adv. Water Resources **31**(2), 219–232 (2008). https://doi.org/10.1016/j.advwatres.2007.08.001

Srinivasan, V., Clement, T.P., Lee, K.K.: Domenico solution—Is it valid? Groundwater **45**(2), 136–146 (2007). https://doi.org/10.1111/j.1745-6584.2006.00281.x

van Genuchten, M.T.: Analytical solutions of the one-dimensional convective-dispersive solute transport equation. Technical Report 1661, United States Department of Agriculture, Agricultural Research Service (1982)

van Genuchten, M.T.: Convective-dispersive transport of solutes involved in sequential first-order decay reactions. Comput. Geosci. **11**(2), 129–147 (1985). https://doi.org/10.1016/0098-3004(85)90003-2

van Genuchten, M.T.: Analytical solutions for chemical transport with simultaneous adsorption, zero-order production, and first-order decay. J. Hydrol. **49**(3), 213–233 (1981). https://doi.org/10.1016/0022-1694(81)90214-6

Wang, H., Wu, H.: Analytical solutions of three-dimensional contaminant transport in uniform flow field in porous media: A library. Front. Environ. Sci. Eng. China **3**(1), 112–128 (2009). https://doi.org/10.1007/s11783-008-0067-z

Wang, H., Han, R., Zhao, Y., Lu, W., Zhang, Y.: Stepwise superposition approximation approach for analytical solutions with non-zero initial concentration using existing solutions of zero initial concentration in contaminant transport. J. Environ. Sci. **23**(6), 923–930 (2011). https://doi.org/10.1016/s1001-0742(10)60486-x

West, M., Kueper, B.: Natural attenuation of solute plumes in bedded fractured rock. In: Proceedings of the US EPA/NGWA Fractured Rock Conference: State of Science and Measuring Success in Remediation. National Ground Water Association, NGWA Press (2004)

West, M.R., Kueper, B.H., Ungs, M.J.: On the use and error of approximation in the Domenico (1987) solution. Groundwater **45**(2), 126–135 (2007). https://doi.org/10.1111/j.1745-6584.2006.00280.x

Wexler, E.J.: Analytical solution for one-, two-, and three-dimensional solute transport in ground-water systems with uniform flow. Technical report, 89–56, USGS (1992). https://doi.org/10.3133/ofr8956

Wilson, J.L., Miller, P.J.: Two-dimensional plume in uniform ground-water flow. J. Hydraulics Div. **104**(4), 503–514 (1978). https://doi.org/10.1061/JYCEAJ.0004975

Xu, M., Eckstein, Y.: Use of weighted least-squares method in evaluation of the relationship between dispersivity and field scale. Groundwater **33**(6), 905–908 (1995). https://doi.org/10.1111/j.1745-6584.1995.tb00035.x

Yeh, G. T. AT123D: Analytical transient one-, two-, and three-dimensional simulation of waste transport in the aquifer system. Technical report, ORNL-5602 ,Oak Ridge National Lab., TN (USA) (1981). https://doi.org/10.2172/6531241